

Sorption of small molecule vapours by single crystals of [Pt{4'-(Ph)trpy}(NCS)]SbF₆ where trpy = 2,2':6',2''-terpyridine: a porous material with a structure stabilised by extended π - π interactions†

John S. Field,* Orde Q. Munro and Bradley P. Waldron

Received 12th December 2011, Accepted 5th March 2012

DOI: 10.1039/c2dt12398c

Treatment of [Pt{4'-(Ph)trpy}Cl]SbF₆ with AgSCN in a metathesis reaction in refluxing acetonitrile affords, after work-up, single crystals of [Pt{4'-(Ph)trpy}(NCS)]SbF₆·CH₃CN, where trpy is 2,2':6',2''-terpyridine. These crystals lose solvent to give single crystals of [Pt{4'-(Ph)trpy}(NCS)]SbF₆ (**1**). An X-ray crystal structure determination of **1** shows that the SCN⁻ ion is N-bound and that the cation as a whole is approximately planar. Compound **1** is porous with “empty” channels that corkscrew through the crystal: this crystal structure is stabilised by extended π - π interactions between the planar cations. When a single crystal of **1** is exposed to vapours of acetonitrile the vapours are sorbed without loss of single crystallinity, as confirmed by crystal structure determinations of **1** and **1**·CH₃CN using the same single crystal. Similarly, single crystals of **1** sorb vapours of methanol without loss of single crystallinity, as confirmed by a crystal structure determination of **1**·CH₃OH. We also report the crystal structure of **1**·(CH₃)₂CO; however, in this case the single crystal was grown directly from acetone. Compound **1** and its solvates are all yellow. Nevertheless, there are differences between the emission spectra recorded for **1** and its solvates in the solid state. Thus, whereas **1** exhibits very weak multiple emission from ³MLCT (MLCT = metal-to-ligand charge transfer) and excimeric ³ π - π * excited states, **1**·CH₃CN and **1**·(CH₃)₂CO both exhibit more intense ³MLCT emission; and the emission by **1**·CH₃OH is complicated by the presence of metallophilic interactions in the crystal. We discuss the role of the solvent in causing these differences.

Introduction

Porous metal-organic framework (MOF) materials are constructed on the principle that metal ions linked by bridging organic ligands provide a reticular framework that encapsulates pores (or voids) in the solid.¹ A host of materials of this type has been investigated because of their potential applications in catalysis,² hydrogen (and other gas) storage,³ luminescent sensor devices,⁴ magnetic materials,⁵ and non-linear optical materials.⁶ There are examples of materials of this type where the reticular framework of covalent bonds is supported by (weaker) intermolecular interactions such as hydrogen bonding,⁷ and extended aromatic interactions;⁸ the latter are usually labeled as “ π - π interactions”.^{9,10} A second group of molecular materials relies on the principles of self-assembly of organic or coordination compounds to construct supramolecular systems that are porous.¹¹

Many of these exhibit a spectroscopic response to the inclusion of small gaseous molecules, a recent example being the supramolecular luminescent system based on 2-cyano-3{4-(diphenylamino)phenyl} acrylic acid, which acts as a selective acetonitrile sensor.¹² The system that we describe here is also molecular and porous with sensing properties, but it has a crystal structure that does not fit into any of the above categories. Instead, the compound [Pt{4'-(Ph)trpy}(NCS)]SbF₆ (**1**) where trpy is 2,2':6',2''-terpyridine, has an open microporous structure containing 2-dimensional stacks of planar [Pt{4'-(Ph)trpy}Cl]⁺ cations that are stabilised solely by extended π - π interactions.

To test the availability of the microporous space in **1** for guest molecule inclusion, we have exposed single crystals of the compound to vapours of acetonitrile, methanol and acetone. Acetonitrile and methanol are sorbed without loss of the single crystallinity but the larger acetone molecule, though sorbed, does disrupt the long range order in the crystal. We also report the photoluminescent properties of **1** and its acetonitrile, methanol and acetone solvates. These materials are all yellow in colour, yet there are differences in their emission spectra, an observation that is relevant to studies of the solid state photophysical properties of terpyridyl ligand complexes of platinum(II).^{13–23}

School of Chemistry, University of KwaZulu-Natal, Private Bag X01, Pietermaritzburg, 3201, South Africa. E-mail: fieldj@ukzn.ac.za

† Electronic supplementary information (ESI) available: X-ray structures of **1_1st**, **1_2nd**, **1_3rd**, **1**·CH₃CN, **1**·CH₃OH and **1**·(CH₃)₂CO. CCDC 857048–857053. For ESI and crystallographic data in CIF or other electronic format see DOI: 10.1039/c2dt12398c

Experimental

Materials and methods

The acetonitrile for the syntheses, crystal growth and for generating vapours was of the Chromosolv™ HPLC grade from Aldrich and used as received. The diethyl ether was from Saarchem and of the uniLAB™ grade and also used as received. The acetone and methanol used for generating vapours were of ACS grade from Aldrich and used as received. The [Pt{4'-(Ph)trpy}Cl]SbF₆ precursor was synthesised by the method described in ref. 22. The AgSCN was obtained from Aldrich and used as received.

[Pt{4'-(Ph)trpy}(NCS)]SbF₆ (1). To a suspension of [Pt{4'-(Ph)trpy}Cl]SbF₆ (100 mg, 0.129 mmol) in acetonitrile (10 mL) was added a suspension of a 10% molar excess of AgSCN (24 mg) in acetonitrile (40 mL). The mixture was heated to reflux for 24 h. After cooling to room temperature the resulting AgCl precipitate was removed by cannular filtration, and the volume of the solvent was reduced *in vacuo*. The concentrated acetonitrile solution was transferred to the lower compartment of a dual chamber purpose-built apparatus; diethyl ether was added to the upper compartment. Slow vapour diffusion of diethyl ether into the concentrated acetonitrile solution resulted in the formation of yellow crystals over a period of ~7 d. These are crystals of the acetonitrile solvate, [Pt{4'-(Ph)trpy}(NCS)]SbF₆·CH₃CN. The yellow crystals were isolated by decantation of the mother liquor, and then washed with small amounts of cold acetonitrile followed by diethyl ether. Allowing the crystalline material to stand in air affords the de-solvated compound, which is also yellow. In order to ensure that all the acetonitrile solvent is lost from the crystals, they were exposed to air for a full week: however, the de-solvation process can be speeded-up by the application of a vacuum. Analytical and spectroscopic data are as follows. [Pt{4'-(Ph)trpy}(NCS)]SbF₆: Yield 71 mg (69%). Colour, yellow. Anal. calcd for C₂₂H₁₅N₄F₆PtSb·H₂O (FW = 816.30 g mol⁻¹): C, 32.37; H, 2.10; N, 6.86. Found: C, 32.21; H, 1.95; N, 6.57%. IR (KBr, cm⁻¹): ν[SC≡N]: 2095s; ν[S–CN]: 866m; ν[4'-(Ph)trpy]: 1610s, 1557ms, 1479ms, 1418s, 881m; ν[SbF₆⁻]: 656vs. ESI MS: *m/z* (relative intensity, ion): 562.0670 (100, M²⁺). ¹H NMR (CD₃CN): δ 8.51 (4H, m, H_{6/6'}, _{3/5'}); 8.42 (4H, m, H_{3/3'}, _{2''/6''}); 8.05 (1H, m, H_{4''}); 7.83 (2H, q, H_{4/4''}); 7.71 (4H, m, H_{5/5''}, _{3'''/5'''}). ¹³C NMR (CD₃CN): δ 157.8 (2C, s, quat.C_{2/2''}); 155.5 (2C, s, quat.C_{2/6'}); 154.7 (1C, s, quat.C_{1''}); 152.2 (2C, s, C_{6/6''}); 142.9 (2C, s, C_{2''/6''}); 142.4 (1C, s, quat.C₄); 131.7 (2C, s, C_{3'''/5'''}); 129.7 (4C, s, C_{5/5'',4/4''}); 128.0 (1C, s, C_{4''}); 125.8 (2C, s, C_{3/3''}); 122.1 (2C, s, C_{3/5'}). UV-vis (1 μM in MeCN): λ_{max}/nm (ε, M⁻¹ cm⁻¹): 409 (20 563); 387 (17 055); 333 (46 406); 319 (49 463); 304 (49 888); 290 (75 511); 282 (68 701); 273 (63 785); 259 (64 492).

Characterisation. Elemental analyses were determined by Galbraith Laboratories of Knoxville, Tennessee, USA. The powder XRD spectrum of **1** was recorded at 295 K with a Philips PW1050 diffractometer using monochromated CoKα radiation (λ = 1.7902 Å) from 3 to 40° in 2θ with a scanning

step of 0.02° at a 1° per minute counting interval. Fourier transform infrared (FTIR) spectra were measured using a Perkin Elmer Spectrum One spectrometer, and the samples prepared as KBr pellets. UV-vis absorption spectra were recorded at 22 °C using a Perkin-Elmer Lambda 45 UV-vis spectrometer. ¹H (500 MHz) and ¹³C (125 MHz) NMR spectra were recorded at 30 °C in CD₃CN on a Bruker Avance III 500 MHz spectrometer with chemical shifts referenced to the solvent.

Emission measurements

The instrument used for the measurement of emission spectra was a Photon Technologies Int. (PTI) fluorescence spectrometer controlled by PTI's Felix32© Version 1.1 software.²⁶ Steady state emission spectra were recorded using PTI's XenoFlash™ 300 Hz pulsed light source and gated emission scans with a delay of 95 ms, an integration window time of 100 ms and 50 pulses per channel (shots). Detection was by means of PTI's Model 814 Analog/Photon-Counting Photomultiplier Detector. The excitation wavelength was 420 nm for all the solid state samples; with the scattered light being removed by means of a suitable wavelength band-pass filter. The spectra are uncorrected for instrument response. For the lifetime measurements, the excitation source was again the Xenon flash lamp (set at 420 nm) with the emission decay captured by the Photomultiplier Detector at a wavelength corresponding to the peak of interest, and analysed by the FeliX32™ software.²⁶ For the measurements at 77 K a PTI-supplied quartz cold finger filled with liquid nitrogen was used to hold the sample tube.

The sample of **1** used for the emission measurements was obtained by crushing single crystals of the compound and thoroughly mixing the powder with finely divided anhydrous KBr to give a 10% (w/w) solid solution. To ensure that any vestiges of water in the sample were removed, the sample was subjected to a high vacuum for several days. The sample was transferred under dry argon to a quartz NMR tube with its top half widened to fit a B14 joint, into which a stopcock was inserted thus allowing for both purging of the sample with argon and the introduction into the sample space of the organic vapours *via* cannulae inserted through a septum. Solvent vapours were generated by vigorously bubbling argon through a sealed 100 mL Erlenmeyer flask containing the anhydrous solvent, and transferred to the sample tube *via* cannulae. Total exposure time of the sample to the stream of solvent vapours was ~60 min. The stopcock was then closed and the sample kept in contact with solvent vapours for a further 3 h. The envelope of solvent vapours was then removed by gently purging with argon and the emission spectrum of the solvated material recorded, at 77 K so as to increase the intensity of the spectrum and to minimise any loss of solvent. For the monitoring experiment the acetonitrile solvate sample was warmed to room temperature and exposed to ambient conditions: emission spectra were then recorded at regular intervals, at 77 K, so ensuring that each spectrum is a “freeze-frame” of the de-solvation process. The emission spectrum of **1** shown in Fig. 10 was obtained in this way, in particular by ensuring that the acetonitrile solvate had de-solvated fully through application of a vacuum.

‡ The chemical shifts listed are for the N-bound isomer that dominates in CD₃CN solution.^{24,25} further details are available from the authors on request.

Single crystal preparations and structure determinations

The first batch of single crystals was isolated by slow vapour diffusion of diethyl ether into an acetonitrile solution of [Pt{4'-(Ph)trpy}(NCS)]SbF₆ (**1**): these were of the acetonitrile solvate, **1**·CH₃CN. Single crystals of **1** itself were obtained by allowing the solvated crystals to lose solvent over a period of about 6 d under ambient conditions: a single crystal was selected from this batch and its structure determined at 200 K. This same crystal (glued to a fibre attached to a brass pin) was transferred to a glass platform by fixing the pin to the platform with Prestik™. The platform was constructed by extending a B24 glass stopper, designed such that when it is inserted through the mouth of a two-necked round bottomed flask, the platform is positioned roughly halfway between the bottom of the flask and the stopper. The flask contained about 20 mL of pure acetonitrile. A gentle vacuum was then applied to the flask and switched off as soon as the solvent began to boil. In this way the crystal was enveloped in vapours of acetonitrile at its vapour pressure at room temperature; in this case the laboratory temperature was ~20 °C and, therefore, the vapour pressure of the acetonitrile was ~43 Torr. The crystal was left exposed to the solvent's vapours for 48 h. After this period, the pin and mounted crystal were removed from the flask and transferred immediately to the diffractometer where it was cooled to 200 K. The temperature of 200 K is a compromise: a low temperature was chosen to minimise solvent loss but dropping the temperature to below 200 K caused the crystal to crack. The data collection for **1**·CH₃CN was done with this crystal. After the data collection was complete, the crystal was warmed to room temperature thus allowing the acetonitrile to evaporate to afford a single crystal of **1**. A second intensity data set, again at 200 K, was collected and the crystal structure of **1** re-determined: see CCDC 857049 in the ESI.† With methanol the same procedure was followed in order to obtain a single crystal and hence an intensity data set for the solvate, **1**·CH₃OH. However, a different starting single crystal of **1** was used and, of course, the vapour pressure of the methanol is different *i.e.* ~125 Torr (with the methanol solvate a temperature of 180 K was used for the data collection). The same procedure was also used for the acetone solvate, using a different starting single crystal of **1** that was exposed to acetone vapours at a pressure of ~230 Torr. Intensity data collected on this crystal gave a structure solution that showed the inclusion of the acetone molecule in the crystal of **1**, see the CheckCIF report in the ESI.† However, with a high final R factor of 10% and problems with thermal motion, the structure determination is not sufficiently accurate to allow for a detailed comparison of geometric parameters between the three solvates and **1**. For this reason we grew a good quality crystal of **1**·(CH₃)₂CO by slow vapour diffusion of diethyl ether into an acetone solution of **1**. This is the structure, determined at 200 K, discussed in the text below. As a final experiment, this same single crystal of **1**·(CH₃)₂CO was warmed to room temperature thus allowing the acetone to evaporate to afford a single crystal of **1**: see CCDC 857050 in the ESI† for details of the structure determination.

Intensity data were collected on an Oxford Diffraction Xcalibur 2 CCD diffractometer in the range $2 \leq \theta \leq 25^\circ$ using graphite-monochromated Mo-K α radiation ($\lambda = 0.71073 \text{ \AA}$). Intensities were corrected semi-empirically for absorption, based

on symmetry-equivalent and repeated reflections. The structures were solved by Patterson methods and refined on F^2 values for all unique data; Table 1 gives further details. All non-hydrogen atoms were refined anisotropically, and H atoms were constrained with a riding model; $U(\text{H})$ was set at 1.2 times (1.5 times in the case of a methyl group) U_{eq} for the parent carbon atom. The programs used were Oxford Diffraction CrystalRED v. 170 (control and data reduction),²⁷ SHELXS-97 and SHELXL-97 (structure solution and refinement);²⁸ for the molecular graphics the programs ORTEP^{32,29} and X-SEED^{30a} were used.

Results and discussion

Treatment of a solution of [Pt{4'-(Ph)trpy}Cl]SbF₆ in refluxing acetonitrile, with one equivalent of silver thiocyanate, afforded *via* a metathesis reaction a precipitate of silver chloride and a solution of [Pt{4'-(Ph)trpy}(NCS)]SbF₆ (**1**). After removal of the AgCl by filtration, the acetonitrile filtrate was concentrated, cooled and transferred to a two compartment vapour diffusion apparatus. Slow diffusion of diethyl ether into the concentrated solution led to the precipitation of a mass of yellow, and mostly single, crystals of the acetonitrile solvate, **1**·CH₃CN. Application of a vacuum to the crystals extricates the solvent, finally affording compound **1**, also as a mass of yellow, and mostly single, crystals. The infrared spectrum recorded as a KBr pellet exhibits a strong sharp peak at 2102 cm⁻¹ assigned to the $\nu(\text{SC}\equiv\text{N})$ stretching mode and a weaker, somewhat broader peak at 866 cm⁻¹, due to the $\nu(\text{S}-\text{CN})$ stretching mode. These stretching frequencies are consistent with a SCN⁻ ion bound to the Pt atom through the N atom in the solid state *i.e.* as the isothiocyanate ligand.^{31–33}

Crystal structure of [Pt{4'-(Ph)trpy}(NCS)]SbF₆ (**1**)

The single crystal of **1** was obtained by exposing crystals of the acetonitrile solvate to ambient conditions for a period of 6 d. Note that the de-solvation process can be speeded up to 1 d by application of a vacuum, again without loss of single crystallinity. A temperature of 200 K was used for the data collection so as to correlate with the temperatures used for the crystal structure determinations of the solvates. Fig. 1 gives a perspective view of the cation in **1**. Selected geometric parameters for the cation are given in Table 2.

The bond distances and angles associated with the Pt(trpy) unit agree well with those obtained from crystal structure determinations of other platinum terpyridine complexes reported in

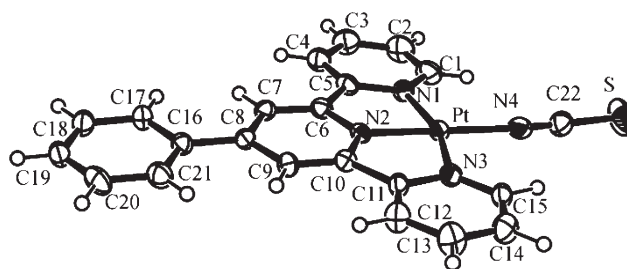


Fig. 1 ORTEP diagram (50% ellipsoids) of the cation in **1**.

Table 1 Crystal structure and refinement data

Compound	1 ^a	1 ·CH ₃ CN ^b	1 ·CH ₃ OH ^c	1 ·(CH ₃) ₂ CO ^d
Empirical formula	C ₂₂ H ₁₅ F ₆ N ₄ PtSSb	C ₂₄ H ₁₈ F ₆ N ₅ PtSSb	C ₂₃ H ₁₉ F ₆ N ₄ OPtSSb	C ₂₅ H ₂₁ F ₆ N ₄ OPtSSb
<i>M_r</i>	798.28	839.33	830.32	856.36
Crystal size/mm	0.15 × 0.25 × 0.60	0.15 × 0.25 × 0.60	0.15 × 0.22 × 0.55	0.10 × 0.20 × 0.30
<i>T</i> /K	200	200	180	200
<i>λ</i> /Å	0.71073	0.71073	0.71073	0.71073
Crystal system	Monoclinic	Monoclinic	Monoclinic	Monoclinic
Space group	<i>P</i> 2 ₁ / <i>n</i>	<i>P</i> 2 ₁ / <i>n</i>	<i>P</i> 2 ₁ / <i>n</i>	<i>P</i> 2 ₁ / <i>n</i>
<i>a</i> /Å	9.6158(2)	9.9301(2)	9.7239(3)	9.7859(3)
<i>b</i> /Å	25.6118(7)	25.7960(9)	25.4860(7)	25.3897(8)
<i>c</i> /Å	10.3103(3)	10.347(3)	10.4632(3)	10.9182(4)
<i>α</i> (°)	90	90	90	90
<i>β</i> (°)	96.392(2)	100.060(2)	98.004(2)	98.355(3)
<i>γ</i> (°)	90	90	90	90
<i>V</i> /Å ³	2523.4(1)	2609.7(8)	2567.8(1)	2684.0(2)
<i>Z</i>	4	4	4	4
<i>D_c</i> /g cm ⁻³	2.101	2.136	2.148	2.119
<i>μ</i> /mm ⁻¹	6.753	6.537	6.644	6.360
<i>F</i> (000)	1496	1584	1568	1624
<i>θ</i> Range (°)	2–25	2–25	2–25	2–25
Reflections collected (independent)	40 442 (9037)	38 184 (8961)	41 513 (9434)	28 462 (5291)
Observed [<i>I</i> > 2σ(<i>I</i>)]	6857	5626	6588	5224
<i>R</i> _{int}	0.0317	0.0423	0.0395	0.0338
No. refined parameters (restraints)	316 (0)	344 (0)	339 (2)	352 (0)
Final <i>R</i> ₁ [<i>I</i> > 2σ(<i>I</i>)]	0.0369	0.0803	0.0373	0.0865
Final <i>wR</i> ₂ (all data)	0.0821	0.2107	0.0862	0.1643
Max, min Δρ/e Å ⁻³	1.86, −1.51	5.66, −4.63	3.02, −2.30	3.36, −3.30

^a Crystal selected from the batch of crystals obtained after allowing acetonitrile to evaporate from the crystals of **1**·CH₃CN that originally formed in the crystal growth chamber: see **1_1st**: CCDC 857048. ^b Crystal obtained by exposing **1_1st** to vapours of acetonitrile. ^c Crystal obtained by exposing a different single crystal of **1** to vapours of methanol. ^d Crystal grown directly from acetone.

Table 2 Selected geometric parameters for the cations in **1** and its solvates (Å/°)

Compound	1	1 ·CH ₃ CN	1 ·CH ₃ OH	1 ·(CH ₃) ₂ CO
Temperature/K	200	200	180	200
Pt–N1	2.022(4)	2.00(1)	2.010(3)	2.02(1)
Pt–N2	1.925(3)	1.920(8)	1.923(3)	1.93(1)
Pt–N3	2.019(4)	2.01(1)	2.016(3)	2.02(1)
Pt–N4	2.023(4)	1.996(9)	2.014(3)	2.01(1)
N4–C22	1.098(6)	1.13(1)	1.120(5)	1.11(2)
C22–S	1.629(5)	1.63(1)	1.623(5)	1.64(2)
N1–Pt–N2	80.7(1)	81.0(4)	81.5(1)	81.6(5)
N1–Pt–N3	162.1(1)	162.8(4)	162.4(1)	162.6(5)
N1–Pt–N4	98.9(1)	98.8(4)	98.5(1)	98.6(5)
N2–Pt–N3	81.3(1)	81.9(4)	80.9(1)	81.0(5)
N2–Pt–N4	179.6(2)	179.7(4)	179.2(1)	179.1(5)
N3–Pt–N4	99.0(2)	98.4(4)	99.1(1)	98.8(5)
Pt–N4–C22	173.1(4)	175.2(9)	175.7(4)	175.1(1)
N4–C22–S	179.5(5)	177(1)	179.2(5)	180(2)

the literature.^{13–23} For example, the irregular square-planar geometry about the platinum atom is reflected in a N1–Pt–N3 ‘*trans*’ angle of 162.1(1)°, and a platinum to central nitrogen distance that is significantly shorter than the distances of the platinum to the two outer pyridine nitrogen atoms. The SCN[−] ion is bound to the platinum through the N atom with a Pt–N4–C22 angle of 173.1(4)° and a N4–C22–S angle of 179.5(5)°. These angles, as well as the N4–C22 and C22–S distances of 1.098(6) and 1.629(5) Å, respectively, are typical of a SCN[−] ion bound to a metal through the N atom.³⁴ Of particular interest is that the phenyl ring is very nearly coplanar with the mean plane through

the trpy moiety, as is reflected in a dihedral angle between the phenyl ring and the central pyridine ring of only 3.1(1)°; in fact, the cation as a whole is essentially planar. This is not an expected result in view of a consequent very short intramolecular H7...H17 non-bonded contact of 2.00 Å, a value that is ~0.4 Å less than the sum of the van der Waals radii for two hydrogen atoms.³⁵ Indeed, a crystal structure determination of the free 4’-(Ph)trpy ligand shows that the phenyl group twists out of the plane of the trpy moiety by 10.9°.³⁶ On the other hand, two previous reports of crystal structure determinations of complexes containing the 4’-(Ph)trpy ligand show that the out-of-plane twist of the phenyl group is variable; thus whereas the relevant torsion angle is 33.4° in [Pt{4’-(Ph)trpy}Cl]BF₄·CH₃CN,²² it is only 1.9° in [Pt{4’-(Ph)trpy}(CN)]BF₄·CH₃CN.³⁷ Clearly, crystal packing forces play a key role in determining the exact extent to which the phenyl group twists out of the plane of the trpy moiety.

A view down the [*c*]-axis of the unit cell contents in **1** is given in Fig. 2; note that this view is chosen since it is approximately perpendicular to the mean plane through the non-H atoms of the cation, henceforth labeled the ‘cation plane’. This view shows that the [Pt{4’-(Ph)trpy}(NCS)]⁺ cations stack separately from the SbF₆[−] anions, but not in one-dimensional columns parallel to the [*c*]-axis. Instead, the cations slot together to give a stack of constant thickness, but which extends along the [*a*]- and [*c*]-axes; as shown in Fig. 2 these stacks repeat at half-intervals along the [*b*]-axis and are separated by the anions. To discuss the nature of the interactions between the cations within a stack we refer to Fig. 3; in this view the cations within one stack are viewed side-on, specifically along the longer [*b*]-axis. By

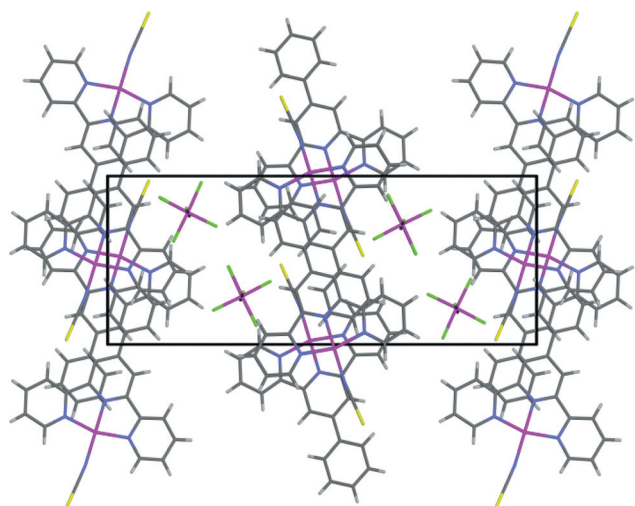


Fig. 2 View down the $[c]$ -axis of the unit cell contents in **1**. The $[a]$ -axis points down the page and the $[b]$ -axis across the page.

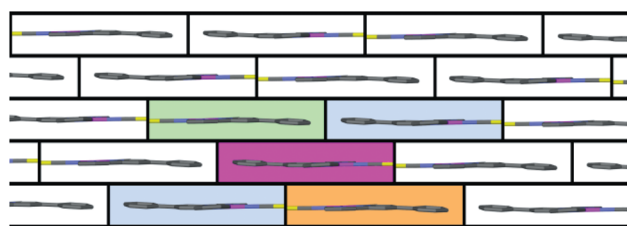


Fig. 3 Side view along the $[b]$ -axis of the "brick-in-wall" packing arrangement of the cations in **1**. Hydrogen atoms have been omitted for clarity. The "bricks" are coloured according to the nature of the interaction of a cation with the central "pink" cation, see text.

focusing on one cation within the stack (colour coded pink) we arrive at the following description of the various cation–cation interactions. This cation is attracted to four nearest neighbour cations, two above (colour coded green and blue) and two below (colour coded blue and orange) with three unique pair-wise interactions: pink-to-green, pink-to-blue and pink-to-orange. These unique interactions are highlighted in Fig. 4, using the same colour coding but applied to the borders and taking a view perpendicular to the cation planes. In Fig. 4(A) (pink-to-orange) the two cations are laterally offset such that π – π overlap occurs at the edges of both outer pyridine rings for the two adjacent trpy moieties; as noted by Hunter and Sanders⁹ and by Janiak¹⁰ this has as a result that π – σ attractive forces dominate between the two aromatic rings. Consistent with this is that the perpendicular distance between the cation planes (the interplanar spacing) is 3.38 Å, a value that has been calculated to be optimal for a stabilising interaction between adjacent aromatic species.^{9,10} On the other hand, the Pt...Pt distance of 3.553(1) Å is too long to support a metallophilic $d_{z^2}(\text{Pt})$ – $d_{z^2}(\text{Pt})$ orbital interaction.³⁸ In Fig. 4(B) (pink-to-green) the cations are laterally and longitudinally offset such that overlap now occurs (twice) between the phenyl and central pyridine rings of the two cations. Again, this overlap geometry favours a stabilising π – π interaction.^{9,10} The Pt...Pt distance is now much longer at 11.757(1) Å, but the

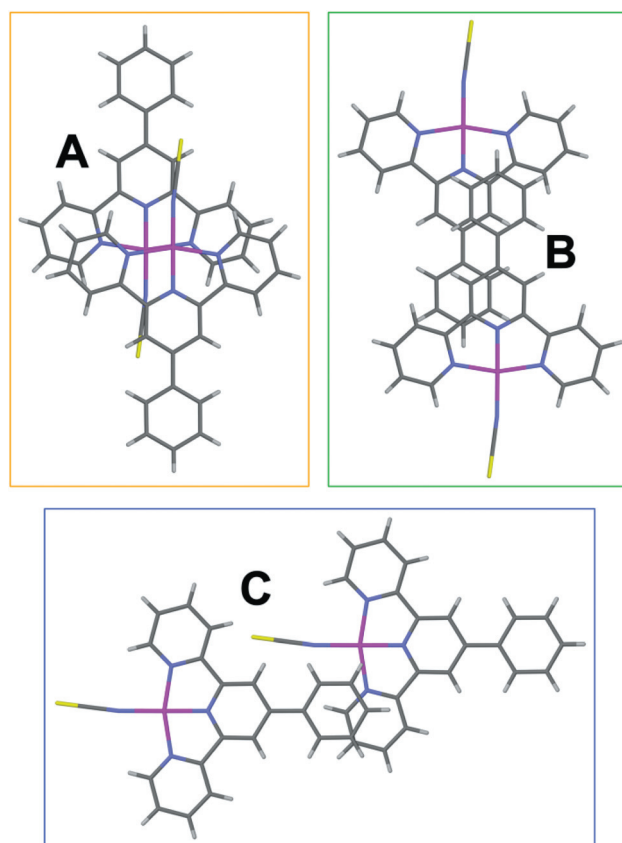


Fig. 4 Views perpendicular to the cation planes for each of the three different types of cation–cation interaction in **1**, see text. In (A) the Pt...Pt distance is 3.553 Å, in (B) 11.757 Å, and in (C) 9.616 Å.

interplanar spacing of 3.34 Å is short enough to support a stabilising π – π interaction: usually 3.8 Å is taken as the upper distance limit for this kind of interaction between planar aromatic species.^{9,10} Finally, in Fig. 4(C) (pink-to-blue) the cations are displaced with respect to each other to such an extent that the only overlap is one between the leading edges of the phenyl ring of one cation and the outer pyridine ring of the adjacent cation. This overlap geometry also supports a stabilising π – π interaction as does the interplanar spacing of 3.27 Å;^{9,10} the Pt...Pt distance is now 9.616(1) Å, clearly too long to support a metallophilic $d_{z^2}(\text{Pt})$ – $d_{z^2}(\text{Pt})$ orbital interaction.³⁸ In summary, the cations within a stack are held together by extended stabilising π – π interactions, while the crystal as a whole is stabilised by attractive electrostatic forces between the positively charged stacks and the SbF_6^- anions that are interspersed between them.

As already noted, de-solvation of a single crystal of the acetonitrile solvate, **1**·CH₃CN, proceeds without loss of the single crystallinity to give the single crystal of **1** with the structure described above. The net result is that the crystal structure of **1** contains solvent accessible voids. Using the MSROLL interface of the program X-SEED,³⁰ we estimate that the voids occupy a volume of 320 Å³ in the unit cell, *i.e.* ca. 13% of the total unit cell volume of 2523 Å³ measured at 200 K. In order to show the location of the voids we have plotted the Connolly surface for **1** using a probe radius of 1.2 Å;³⁹ three different views of the surface are shown in Fig. 5. In views (A) and (B) the corkscrew

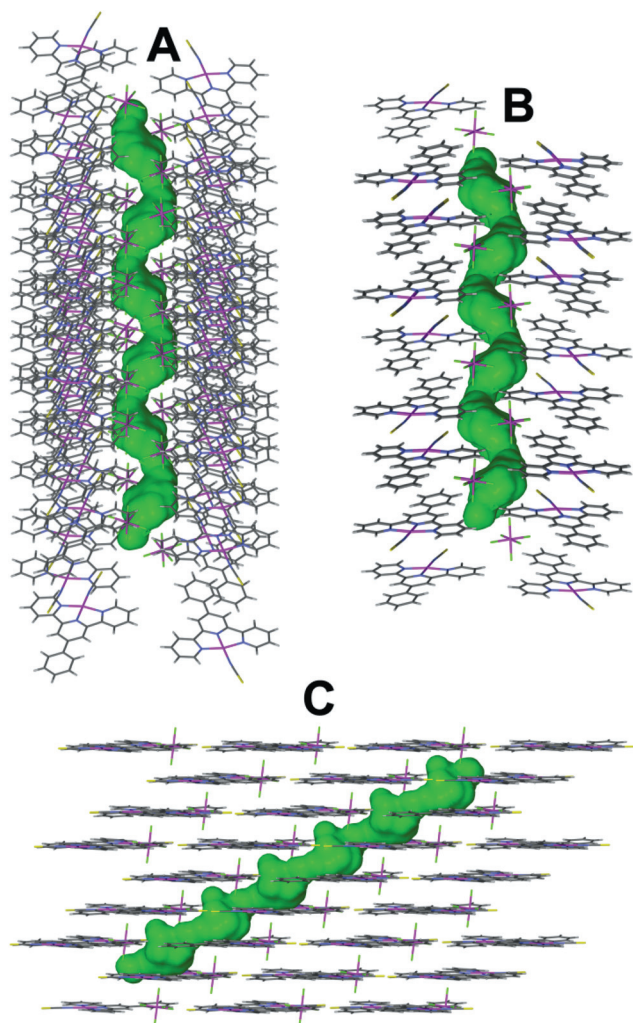


Fig. 5 Three different views of the solvent accessible voids in **1** shown as green Connolly surfaces drawn with a probe radius of 1.2 Å.³⁹ In (A) and (B) the “corkscrew” motif for the Connolly surface is emphasised while view (C) shows the bulges that are connected by narrower channels.

shape of the channels that extend through the crystal is apparent, while view (C) shows that the channels are not of uniform cross-section, but rather comprise narrow sections that connect larger bulges. It is these larger bulges that accommodate molecules of acetonitrile, methanol and acetone in the corresponding solvates, **1**·CH₃CN, **1**·CH₃OH and **1**·(CH₃)₂CO. We now discuss the uptake of vapours of these solvents by single crystals of **1**.

Crystal structures of **1**·CH₃CN, **1**·CH₃OH and **1**·(CH₃)₂CO

The intensity data for the crystal structure determinations of the three solvates were collected at low temperatures in order to slow down the loss of solvent that occurs quite rapidly at room temperature. The actual temperatures used were a compromise: dropping the temperature too low caused the crystals to crack. The single crystal used for the determination of the structure of the acetonitrile solvate that we describe here was the *same* one used for the crystal structure determination of **1**, described above.

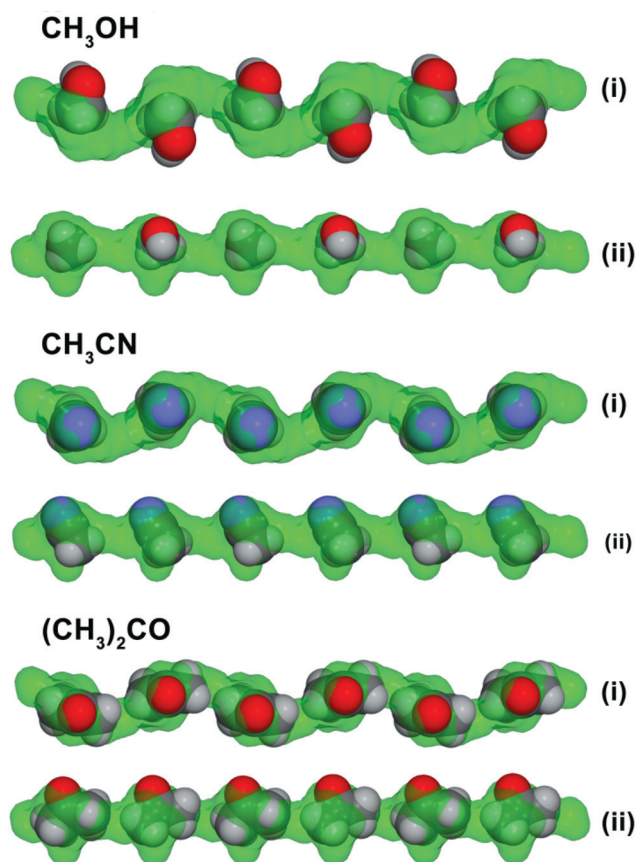


Fig. 6 Plots showing two different views of the location of the solvent molecules in **1**·CH₃CN, **1**·CH₃OH, and **1**·(CH₃)₂CO in relation to the Connolly surface (shown in green) obtained from the crystal structure of **1**.

This crystal was exposed to vapours of acetonitrile at its vapour pressure in a closed container for a period of 48 h during which time the solvent was sorbed by the crystal to afford **1**·CH₃CN, *without* loss of the single crystallinity. During the sorption process the cation π -stacks remain intact with only very small changes to their dimensions; also the SbF₆[−] anion positions determined for **1** hardly change. As a result, the packing of the cations and anions in **1**·CH₃CN (see Fig. S1 in the ESI[†]) appears very similar to the crystal packing illustrated in Fig. 2 for the de-solvated compound, **1**. With regard to the location of the solvent molecules in **1**·CH₃CN, we show in Fig. 6 their positions in relation to the Connolly surface drawn for **1**; as expected, the acetonitrile molecules fit neatly into the bulges of the Connolly surface implying little disruption of the porous crystal structure of **1**. As a result, the internal dimensions and geometry of the cation are much the same as those determined from the crystal structure determination of **1**, see Table 2. More interesting is that there are no unusually short intermolecular contacts between atoms of the acetonitrile molecule and atoms of the cation and anion, *i.e.* there is no evidence from the crystal structure of **1**·CH₃CN for strong binding of the solvent in the lattice, consistent with the ease with which acetonitrile molecules escape the crystal. Indeed, we have shown that this same crystal can undergo loss of solvent for a second time without loss of single crystallinity: see CCDC 857049.†

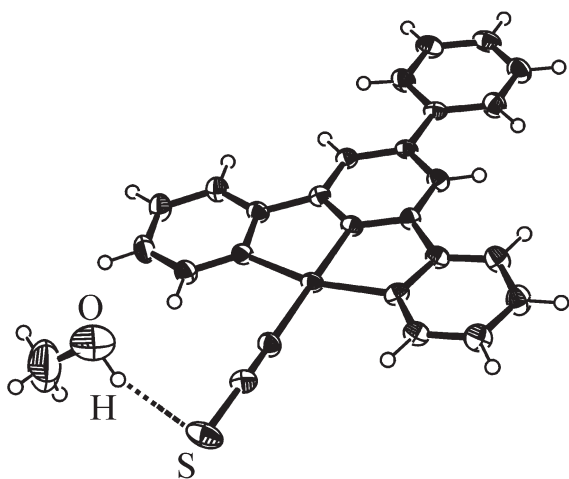


Fig. 7 ORTEP diagram (50% ellipsoids) showing the O–H...S intermolecular contact between the methanol and S atom of the isothiocyanate ligand: O–H = 1.00 Å, O...S = 3.31, S...H = 2.38 Å, O–H...S = 157°.

Turning to the sorption of methanol by single crystals of **1** we find that, though single crystals of **1** can sorb methanol molecules from the vapour phase without loss of single crystallinity, extrication of methanol from the crystal is much more difficult; in fact, the application of a vacuum is required with a concomitant loss of single crystallinity. We are not sure why this is the case, especially as methanol has a higher vapour pressure than acetonitrile, and is a smaller molecule (two non-hydrogen atoms rather than three). Of course, the possibility of hydrogen bonding exists between the methanol and the sulfur atom of the isothiocyanate ligand; and such a bond would make the methanol more difficult to extricate. To investigate this possibility we have checked the shortest intermolecular contacts between the methanol and the sulfur atom, see Fig. 7 and its caption, which gives these parameters. In fact, the dimensions given do not suggest the presence of an O–H...S hydrogen bond,⁴⁰ for example the O...S distance simply fits with the sum of the van der Waals radii for the two atoms concerned.³⁵ However, the methanol is oriented with respect to the sulfur atom such that even a very small shift of atom positions could lead to the formation of a hydrogen bond – perhaps this happens when attempts are made to remove the methanol. Turning to the overall packing in this solvate we first note that there are no obvious differences in the positions of the cation and anions as compared to those in **1** and in the acetonitrile solvate; compare Fig. S2† with Fig. 2 and Fig. S1.† Consistent with this observation is that the methanol molecules fit neatly into the bulges in the Connolly surface drawn for **1**, see Fig. 6. However, examination of the Pt...Pt distances shows that there is a small but significant effect on these distances (Table 3) the most relevant being on the Pt...Pt distance associated with the cation–cation interaction labeled “A” in Fig. 4. The Pt...Pt(A) distance drops from a value above 3.5 Å for **1** and **1·CH₃CN** to a value of 3.395(1) Å for **1·CH₃OH**, which is below the upper distance limit of ~3.5 Å usually taken to indicate a finite $d_{z^2}(\text{Pt})$ – $d_{z^2}(\text{Pt})$ orbital interaction.³⁸ As expected, the presence of the metallophilic interaction influences the photophysical properties of the methanol solvate in the solid state, see below.

Table 3 Comparison of the three unique Pt...Pt distances (Å) measured for **1** and its solvates

Compound	1	1·CH₃CN	1·CH₃OH	1·(CH₃)₂CO
Temp (K)	200	200	180	200
Pt...Pt(A) ^a	3.553(1)	3.519(1)	3.395(1)	3.443(1)
Pt...Pt(B) ^a	11.757(1)	11.562(1)	11.754(1)	11.980(1)
Pt...Pt(C) ^a	9.616(1)	9.930(1)	9.724(1)	9.786(1)

^a A, B and C label the distances according to the nature of the cation–cation interaction: see Fig. 4.

Single crystals of **1** have also been exposed to vapours of acetone, which is the largest of the three solvent molecules studied, containing four non-hydrogen atoms. We find that acetone is sorbed, but not without some disruption of long range order in the crystal. Evidence for this comes from a crystal structure determination of the solvate at 200 K. A better crystal of **1·(CH₃)₂CO** was obtained by direct crystallization of the solvate from a solution of **1** in acetone and a more reliable crystal structure determination made. As with the acetonitrile and methanol solvates, a visual comparison of the relevant crystal packing diagrams (Fig. 2 with Fig. S3†) shows no obvious differences in the positions of the cation and anions between the two crystal structures. Consistent with this observation is that the acetone molecules fit neatly into the bulges in the Connolly surface drawn for **1**, see Fig. 6. Noteworthy is that there is no evidence for hydrogen bonding (potential or actual) of the O atom of the acetone to the S atom of the isothiocyanate ligand; in fact, there are no unusually short intermolecular contacts involving the acetone molecules. However, because of the increased size of the acetone molecule, its inclusion in the crystal does have a small effect on the dimensions of the cation stack, in particular on the Pt...Pt distances, see Table 3. The shortest (A) distance of 3.443 (1) Å is now just below the upper distance limit of ~3.5 Å usually taken to indicate a finite $d_{z^2}(\text{Pt})$ – $d_{z^2}(\text{Pt})$ orbital interaction,³⁸ but is not short enough to have any discernable effect on the emission measured for **1·(CH₃)₂CO** in the solid state, see below. In so far as the loss of acetone from a single crystal of **1·(CH₃)₂CO** is concerned, this occurs relatively slowly under ambient conditions (~2 weeks) and there is no concomitant loss of single crystallinity, as confirmed by a crystal structure determination: see CCDC 857050.† The longer de-solvation time is unexpected in view of the high vapor pressure for acetone, certainly higher than that for acetonitrile, which escapes more quickly. We suggest that this has to do with the larger size of the acetone molecule and that because it is larger, it becomes more difficult for the acetone molecules to escape through the narrow channels that link the larger bulges, see Fig. 5.

Emission spectroscopy of solid **1**, **1·CH₃CN**, **1·CH₃OH** and **1·(CH₃)₂CO**

Emission measurements and gas sorption studies were made using a dry powder sample of **1**. An XRD spectrum was recorded on the powder and is compared in Fig. S4 in the ESI† with the powder XRD spectrum calculated using the single crystal data: the excellent agreement suggests that there is no

phase change brought about by crushing the single crystals to give the powder. This powder sample was then mixed with anhydrous KBr to give a 10% (w/w) solid solution – in order to increase the surface area of the sample and so as to speed up gas sorption and de-sorption. The emission spectrum recorded for **1** was found to be extremely weak with no observable signal at room temperature – it was only by lowering the temperature to 77 K that a measurable spectrum could be obtained. In contrast, the emission spectra recorded for the solvates were found to be more intense, in particular those of the acetonitrile and acetone solvates. These observations informed the following sequence in which the gas sorption and emission measurements were done. Dry samples of **1** were first exposed to vapours of acetonitrile and acetone and the emission spectra of the corresponding solvates recorded, at 77 K, in order to minimise any potential loss of solvent and to maximise the intensity of the emission, see Fig. 8 for the emission spectra of **1**·CH₃CN and **1**·(CH₃)₂CO. These are very similar, both comprising three bands at 550, 587 and 632 nm whose intensities decrease monotonically with an increase in wavelength. This envelope of vibronic structure as well as the vibrational spacing of ~1200 cm⁻¹ are a signature for monomeric ³MLCT emission by a platinum terpyridine complex.^{37,41–43} Similar emission lifetimes of ~12 μs at 77 K have been recorded for the emission by both solvates, but the intensity of the emission by the acetonitrile solvate is higher than that for the acetone solvate. In commenting on the ³MLCT emission exhibited by **1**·CH₃CN and **1**·(CH₃)₂CO, we first note that the crystal structures of the two solvates show very similar arrangements for the cations and, therefore, similar emission properties are to be expected. The enhanced intensity of the emission by the acetonitrile solvate as compared to the acetone solvate is presumably to do with slower non-radiative decay of the excited state for the former as compared to the latter *i.e.* k_{nr} for **1**·CH₃CN is $<k_{nr}$ for **1**·(CH₃)₂CO. The magnitude of a k_{nr} value for a solid is usually linked to the extent of thermal vibration by the atoms in the solid.⁴⁴ On this basis, the atoms in the acetone solvate vibrate on average more than the atoms in the acetonitrile solvate, as might be expected since the larger acetone molecules disrupt the efficiency of packing more than the acetonitrile molecules.

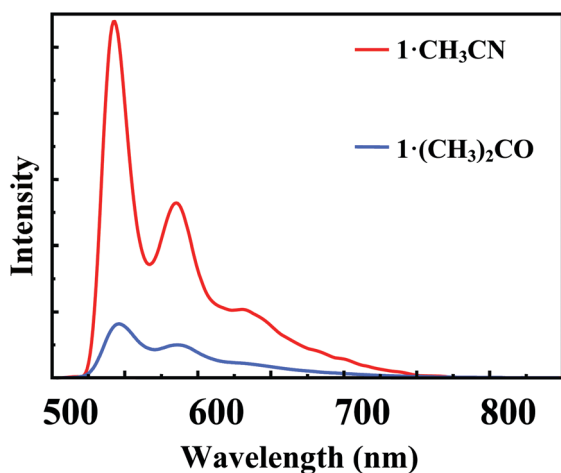


Fig. 8 Emission spectra recorded at 77 K on solid samples of **1**·CH₃CN (red) and **1**·(CH₃)₂CO (blue). λ_{ex} = 420 nm.

The following approach was used in order to obtain a reliable emission spectrum of the de-solvated material, **1**. The emission spectrum of the acetonitrile solvate, **1**·CH₃CN, was recorded following which the sample was exposed to ambient conditions. The loss of solvent was monitored by recording the emission spectrum at regular intervals – at 77 K, so ensuring that each spectrum is a “freeze-frame” of the de-solvation process. The results are shown in Fig. 9. Initially, solvent loss causes the ³MLCT emission to gradually and systematically drop in intensity, *i.e.* the relative intensities of the vibrational components stay the same but the overall (integrated) intensity of the emission drops. However, when the de-solvation process is well-advanced (see the insert spectra) it becomes apparent that while the vibrational components at 550 and ~590 nm continue to drop in intensity, the component at ~650 nm stays much the same in intensity. Eventually, a very weak emission spectrum is obtained that does not change even if the sample is pumped with a high vacuum to remove any vestiges of solvent: this is the 77 K spectrum for the de-solvated compound, **1**, and is shown separately in Fig. 10. As the figure shows, the spectrum consists of a broad band that maximises at 650 nm, with higher energy shoulders at ~550 and ~590 nm. To aid in its interpretation we have determined the emission lifetimes by monitoring the decay in intensity with time of each of the three component peaks. The decay curves determined at 550 and 590 nm are biphasic affording best fit lifetimes of 2.0 and 9.3 μs for the 500 nm peak, and 2.5 and 12.4 μs for the 590 nm peak. In contrast, the decay curve for the dominant 650 nm peak is monophasic with a lifetime of 1.9 μs. These lifetime data suggest that **1** exhibits simultaneous emission from two different excited states, one with $\tau \sim 10 \mu\text{s}$ and the other with $\tau \sim 2 \mu\text{s}$. Since the bands at 550 and 590 nm coincide with the higher energy ³MLCT bands recorded for the two solvates (as shown clearly by the monitoring experiment, see Fig. 9) we assign one emitting state as ³MLCT in origin. Consistent with this assignment is that the lifetime measured independently for the ³MLCT emission by the acetonitrile solvate (~12 μs, *vide supra*) fits with the lifetimes of

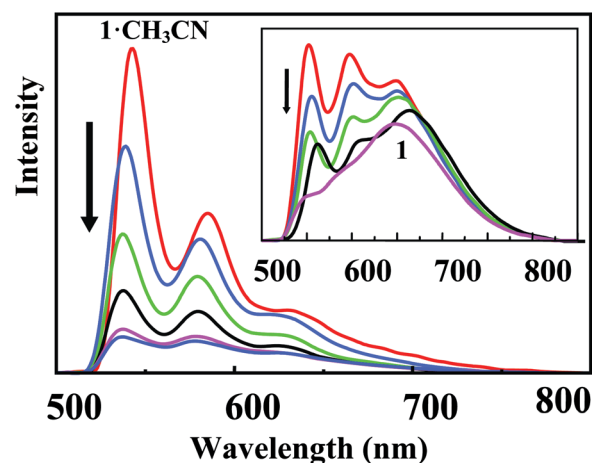


Fig. 9 Emission spectra of various levels of solvation of **1** by acetonitrile, starting with **1**·CH₃CN (red line on main plots) and ending at **1** (purple line on insert plots). The intensities of the spectra are such that the least intense spectrum on the main plots is slightly more intense than the most intense spectrum on the insert plots.

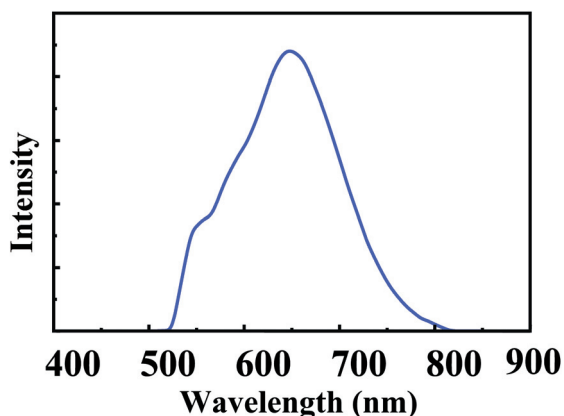


Fig. 10 Emission spectrum of a crystalline powder sample of **1** recorded at 77 K. $\lambda_{\text{ex}} = 420$ nm.

~ 10 μs measured for the 550 and 590 nm bands in the emission spectrum of **1**. We assign the band at 650 nm to emission from an excimeric $^3\pi-\pi^*$ excited state. Consistent with this assignment is that the emission is broad, at lower energy, weak and poorly resolved.^{13,14,17,18,20,45} In summary, irradiation of compound **1** leads to emission from two distinct excited states, one $^3\text{MLCT}$ in origin and other excimeric $^3\pi-\pi^*$ in origin, with the latter more intense than the former.

To conclude the discussion of the emission spectra of the acetonitrile and acetone solvates and of **1**, we make the following observations. As shown in Fig. 9, the $^3\text{MLCT}$ emission that characterises the acetonitrile and acetone solvates systematically drops in intensity as solvent molecules are lost from the solid. The reverse is also true: when a sample of **1** is exposed to vapours of acetonitrile or acetone the $^3\text{MLCT}$ component of the emission systematically intensifies. Note, this does not apply to the excimeric $^3\pi-\pi^*$ component of the emission, which remains very weak whether solvent molecules are present or not. We do not have an explanation for the different responses by the $^3\text{MLCT}$ and excimeric $^3\pi-\pi^*$ emission to small molecule sorption and de-sorption. However, the geometries of the two excited states must be different, and on this basis also the mechanisms of their de-activation: clearly the $^3\text{MLCT}$ state is stabilised to de-activation by the presence of solvent molecules whereas the excimeric $^3\pi-\pi^*$ emission is not. Whatever the precise mechanisms, the result is that the sorption–de-sorption of acetonitrile and acetone by **1** can be easily monitored by emission spectroscopy. In fact, using this approach we have shown that the uptake and loss of these two solvent vapours by a powder sample of **1** can be cycled through indefinitely, specifically at least 10 times. Whether this is in general true, *i.e.* whether sorption–de-sorption of other small molecules will induce the same response, will have to be the subject of further investigations.

The emission spectrum recorded at 77 K for the methanol solvate, **1**·**CH₃OH**, is shown in Fig. 11; at room temperature the emission is barely detectable. The emission is characterised by two distinct peaks, one at 550 nm and another somewhat more intense and rather broad peak at 607 nm. Clearly, the spectrum is very different to the well-defined spectra measured for the acetonitrile and acetone solvates, see Fig. 8. Also different is that the peak separation is ~ 1800 cm^{-1} , a value which falls outside the

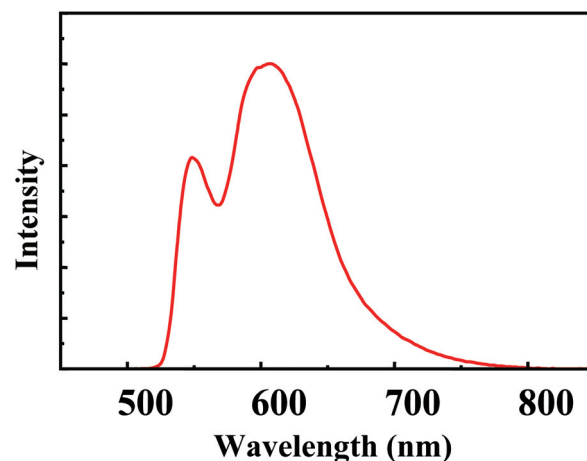


Fig. 11 Emission spectrum recorded at 77 K on a solid sample of **1**·**CH₃OH**. $\lambda_{\text{ex}} = 420$ nm.

normal range of 1200–1400 cm^{-1} for the relevant stretching vibrations of a terpyridyl ligand.^{37,41–43} These observations lead to the inevitable conclusion that the methanol solvate, unlike the acetonitrile and acetone solvates, does not exhibit vibronically structured $^3\text{MLCT}$ emission in the solid state, at least not *solely* $^3\text{MLCT}$ emission. Yet, the peak at 550 nm does coincide with the 550 nm band assigned to the 0–0 component of the $^3\text{MLCT}$ emission by **1**·**CH₃CN** and **1**·(**CH₃)₂CO**, see Fig. 8. To aid in the interpretation of the emission by the methanol solvate we have determined the emission lifetimes by monitoring the decay in intensity with time of each of the two bands. The decay curves determined for the 550 and 607 nm bands are biphasic affording best fit lifetimes of 3.3 and 14.2 ms for the 550 nm band, and 2.3 and 15.5 ms for the 607 nm band, respectively. The longer lifetimes fit approximately with the lifetimes of ~ 12 ms measured for the $^3\text{MLCT}$ emission by the acetonitrile and acetone solvates, further suggesting that there is a $^3\text{MLCT}$ contribution to the emission by the methanol solvate. We now turn our attention to the peak at 607 nm. This peak is significantly blue-shifted and narrower than the peak at 650 nm that was assigned to excimeric $^3\pi-\pi^*$ emission for the de-solvated compound, **1**, see Fig. 10. Therefore, it is highly unlikely that excimeric emission $^3\pi-\pi^*$ is solely responsible for the peak at 607 nm. Thus, the relatively intense peak at 607 nm is new and, being new, leads one to conclude that the peaks at 550 and 607 nm have different origins, *i.e.* **1**·**CH₃OH** exhibits simultaneous emission from (at least) two separate excited states in the solid state.

We now address the question of the origin of the multiple emission by **1**·**CH₃OH**. The crystal structure determination of **1**·**CH₃OH** at 180 K is helpful in this regard, *vide supra*. This structure determination shows that there is a short Pt...Pt distance of 3.395(1) Å linking the two platinum atoms of the pair labeled “A” in Fig. 5, a distance well within the limit of ~ 3.5 Å for a finite $d_{z^2}(\text{Pt})-d_{z^2}(\text{Pt})$ orbital interaction.³⁸ On this basis, we would anticipate that a $^3\text{MMLCT}$ excited state would contribute to the emission by **1**·**CH₃OH** and that, therefore, the “new” peak at 607 nm in Fig. 10 has its origins in $^3\text{MMLCT}$ emission. As already implied, the peak at 550 nm is associated with the monomeric $^3\text{MLCT}$ emission that typifies emission by **1**·**CH₃CN** and

$1 \cdot (\text{CH}_3)_2\text{CO}$. To test this assumption we have de-convoluted the spectrum in Fig. 11 into constituent Gaussian bands using standard non-linear regression methods; the results are shown in Fig. S5.† A total of five bands are mandatory in order to provide a suitable fit of the experimental emission spectrum of the sample. The Gaussian bands coloured blue, light blue and pink are centred at 550, 585 and 631 nm and, moreover, decrease monotonically in intensity as the wavelength increases. This profile, as well as the band energies, match that of the $^3\text{MLCT}$ emission exhibited by $1 \cdot \text{CH}_3\text{CN}$ and $1 \cdot (\text{CH}_3)_2\text{CO}$, see Fig. 8. The fourth band of interest, coloured green, is centred at 609 nm with a fwhm value of 1590 cm^{-1} , *i.e.* it is relatively narrow. This band is, both in terms of energy and profile, typical of the kind of emission exhibited by planar complexes of platinum(II) that have crystal structures containing Pt_2 dimers: see for example $[\text{Pt}(\text{trpy})\text{Cl}]\text{CF}_3\text{SO}_3$ ($\lambda_{\text{em}}^{\text{max}} = 625 \text{ nm}$ at 77 K),¹³ $[(2,6\text{-di-(2'-naphthyl)-4-pyridine})\text{Pt}_2\{\mu\text{-bis(diphenylphosphino)-methane}\}]$ ($\lambda_{\text{em}}^{\text{max}} = 602 \text{ nm}$) and its solvates.⁴⁶ We therefore assign it as $^3\text{MMLCT}$ in origin. Finally, the fifth band, coloured red, is very broad and centered at 652 nm. Of course, this band is reminiscent of the 650 nm band observed in the emission spectrum of the de-solvated compound, **1**, see Fig. 10. We conclude that the emission spectrum of $1 \cdot \text{CH}_3\text{OH}$, though complicated, is understandable in terms of the simultaneous emission from $^3\text{MLCT}$, $^3\text{MMLCT}$ and excimeric $^3\pi\text{-}\pi^*$ excited states.

Conclusions

The crystal structure of **1** is unusual in that it is porous with an open framework that is constructed from repeating 2-dimensional π -stacks of planar $[\text{Pt}\{4'-(\text{Ph})\text{trpy}\}(\text{NCS})]^+$ cations interspersed with SbF_6^- anions; far more common are coordination compounds that are porous but where the open structure comprises a reticular framework of metal ions linked by bridging organic ligands.¹ The π -stacks are stabilised by extended π - π interactions. These involve relatively weak electrostatic forces,^{9,10} yet compound **1** reversibly sorbs and de-sorbs small molecules *without disruption of the open framework structure* – provided, of course, that the intermolecular forces between the molecules and the cations (or anions) are of the weak van der Waals type. Note that this is not true of the closely-related (parent) compound, $[\text{Pt}(\text{trpy})(\text{NCS})]\text{SbF}_6$, for which there is no substituent in the 4'-position of the terpyridyl ligand. This compound is red (not yellow) and also sorbs and de-sorbs small molecules, in particular acetonitrile, pyridine and dimethylformamide.²⁴ However, the sorption–de-sorption process is accompanied by a reversible red-to-yellow colour change. This colour change can be attributed to the breaking and making of metallophilic $\text{Pt}\cdots\text{Pt}$ interactions in the solid state.²⁴ The point is that $[\text{Pt}(\text{trpy})(\text{NCS})]\text{SbF}_6$ has a space-filling crystal structure that is disrupted on small molecule sorption: to be precise, the planar $[\text{Pt}(\text{trpy})(\text{NCS})]^+$ cations slide into new positions when molecules are sorbed or desorbed.²⁴ Clearly this does not apply to the planar $[\text{Pt}\{4'-(\text{Ph})\text{trpy}\}(\text{NCS})]^+$ cations in compound **1** – they hardly move when molecules such as acetonitrile are reversibly sorbed. The reason has to do with the 4'-phenyl substituent, in particular that it participates in a stabilising π - π interaction with the outer pyridine ring of an adjacent cation, see Fig. 4(C). This interaction, not possible for the $[\text{Pt}(\text{trpy})(\text{NCS})]^+$ cation, makes all

the difference – the cations stay in position and do not move when the material is exposed to vapours of small molecules such as acetonitrile. Or, to put it in another way, if acetonitrile is lost from the solvate, $1 \cdot \text{CH}_3\text{CN}$, the cations stay fixed in position and an open porous crystal structure is obtained.

Acknowledgements

The authors thank the South African National Research Foundation and the University of KwaZulu-Natal for financial support. B. P. W. thanks the Department of Labour for a Scarce Skills bursary.

References

- (a) O. M. Yaghi, M. O'Keeffe, N. W. Ockwig, H. K. Chae, M. Eddaoudi and J. Kim, *Nature*, 2003, **423**, 705; (b) A. K. Cheetham, C. N. R. Rao and R. K. Feller, *Chem. Commun.*, 2006, 4780; (c) J. W. Steed and J. L. Atwood, *Supramolecular Chemistry*, Wiley, Chichester, UK, 2009, 2nd edn, pp. 538–589; (d) S. Kitagawa and R. Matsuda, *Coord. Chem. Rev.*, 2007, **251**, 2490.
- P. M. Forster and A. K. Cheetham, *Top. Catal.*, 2003, **24**, 79.
- (a) J. L. C. Roswell, A. R. Millward, K. S. Park and O. M. Yaghi, *J. Am. Chem. Soc.*, 2004, **126**, 5666; (b) T. Duren, L. Sarkisov, O. M. Yaghi and R. Q. Snurr, *Langmuir*, 2004, **20**, 2684; (c) J. L. C. Roswell and O. M. Yaghi, *Angew. Chem., Int. Ed.*, 2005, **44**, 4670; (d) J. A. Rood, B. C. Noll and K. W. Henderson, *Inorg. Chem.*, 2006, **45**, 5521.
- (a) A. de Bettencourt-Dias, *Inorg. Chem.*, 2005, **44**, 2734; (b) X. D. Gou, G. S. Zhu, Q. R. Fang, M. Xue, G. Tian, J. Y. Sun, X. T. Li and S. L. Qiu, *Inorg. Chem.*, 2005, **44**, 3580.
- G. Férey, *Chem. Mater.*, 2001, **13**, 3084.
- (a) K. T. Holman, A. M. Pivovar, J. A. Swift and M. D. Ward, *Acc. Chem. Res.*, 2001, **34**, 107; (b) O. R. Evans and W. B. Lin, *Acc. Chem. Res.*, 2002, **35**, 511.
- K. Uemura, K. Saito, S. Kitagawa and H. Kita, *J. Am. Chem. Soc.*, 2006, **128**, 16416.
- S.-I. Noro, S. Kitagawa, T. Nakamura and T. Wada, *Inorg. Chem.*, 2005, **44**, 3960.
- C. A. Hunter and J. K. M. Sanders, *J. Am. Chem. Soc.*, 1990, **112**, 5525.
- C. Janiak, *J. Chem. Soc., Dalton Trans.*, 2000, 3885.
- (a) B. Chatterjee, J. C. Noveron, M. J. E. Resendiz, J. Liu, T. Yamamoto, D. Parker, M. Cinke, C. V. Nguyen, A. M. Arif and P. J. Stang, *J. Am. Chem. Soc.*, 2004, **126**, 10645; (b) T. Jacobs, J.-A. Gertenbach, D. Dinabandhu and L. J. Barbour, *Aust. J. Chem.*, 2010, **63**, 573; (c) A. W. Kleij, M. Kuil, D. M. Tooke, M. Lutz, A. L. Spek and J. N. H. Reek, *Chem.-Eur. J.*, 2005, **11**, 4743; (d) S.-S. Sun and A. J. J. Lees, *J. Am. Chem. Soc.*, 2000, **122**, 8956; (e) L. Dobrzanska, G. O. Lloyd, H. G. Raubenheimer and L. J. Barbour, *J. Am. Chem. Soc.*, 2005, **127**, 13134; (f) L. Dobrzanska, G. O. Lloyd, H. G. Raubenheimer and L. J. Barbour, *J. Am. Chem. Soc.*, 2006, **128**, 698; (g) L. Dobrzanska, G. O. Lloyd, C. Esterhuysen and L. J. Barbour, *Angew. Chem., Int. Ed.*, 2006, **45**, 5856; (h) S. Belanger, J. T. Hupp, C. L. Stern, R. V. Slone, D. F. Watson and T. G. Carrell, *J. Am. Chem. Soc.*, 1999, **121**, 557; (i) M. Albrecht, M. Lutz, A. L. Spek and G. van Koten, *Nature*, 2000, **406**, 970; (j) Z. Huang, P. S. White and M. Brookhart, *Nature*, 2010, **465**, 598; (k) C. D. Jones, J. C. Tan and G. O. Lloyd, *Chem. Commun.*, 2012, **48**, 2110.
- S. P. Anthony, C. Delaney, L. Varughese, L. Wang and S. M. Draper, *CrystEngComm*, 2011, **13**, 6706.
- H.-K. Yip, L.-K. Cheng, K.-K. Cheung and C.-M. Che, *J. Chem. Soc., Dalton Trans.*, 1993, 2933.
- J. A. Bailey, M. G. Hill, R. E. Marsh, V. M. Miskowski, W. P. Schaefer and H. B. Gray, *Inorg. Chem.*, 1995, **34**, 4591.
- H.-S. Lo, S.-K. Yip, N. Zhu and V. W.-W. Yam, *Dalton Trans.*, 2007, 4386.
- J. S. Field, J.-A. Gertenbach, R. J. Haines, L. P. Ledwaba, N. T. Mashapa, D. R. McMillin, O. Q. Munro and G. C. Summerton, *Dalton Trans.*, 2003, 1176.
- J. S. Field, R. J. Haines, D. R. McMillin and G. C. Summerton, *J. Chem. Soc., Dalton Trans.*, 2002, 1369.

- 18 J. S. Field, L. P. Ledwaba, O. Q. Munro and D. R. McMillin, *CrystEngComm*, 2008, **10**, 740.
- 19 T. J. Wadas, Q.-M. Wang, Y.-J. Kim, C. Flaschenreim, T. N. Blanton and R. Eisenberg, *J. Am. Chem. Soc.*, 2004, **126**, 16841.
- 20 R. Büchner, J. S. Field, R. J. Haines, C. T. Cunningham and D. R. McMillin, *Inorg. Chem.*, 1997, **36**, 3952.
- 21 P. Du, J. Schneider, W. W. Brennessel and R. Eisenberg, *Inorg. Chem.*, 2008, **47**, 69.
- 22 R. Büchner, C. T. Cunningham, J. S. Field, R. J. Haines, D. R. McMillin and G. C. Summerton, *J. Chem. Soc., Dalton Trans.*, 1999, 711.
- 23 R. Büchner, J. S. Field, R. J. Haines, L. P. Ledwaba, R. McGuire Jr., D. R. McMillin and O. Q. Munro, *Inorg. Chim. Acta*, 2007, **360**, 1633.
- 24 J. S. Field, C. D. Grimmer, O. Q. Munro and B. P. Waldron, *Dalton Trans.*, 2010, **39**, 1558.
- 25 B. P. Waldron, *MSc thesis*, University of KwaZulu-Natal, 2009.
- 26 Photon Technologies International, Birmingham, NJ 08011, USA, Felix32© Analysis version 1.1 (build 51 Beta 8), program for the analysis of emission spectra, 2003.
- 27 Oxford Diffraction Ltd., Abingdon, Oxford, OX14 1RL, UK, 2003.
- 28 G. M. Sheldrick, *SHELXS-97 and SHELXL-97*, University of Göttingen, 1997; G. M. Sheldrick, *Acta Crystallogr., Sect. A*, 2008, **64**, 112.
- 29 L. J. Farrugia, ORTEP3 for Windows, Department of Chemistry, University of Glasgow, Glasgow, G12 8QQ, UK, 2001; L. J. Farrugia, *J. Appl. Crystallogr.*, 1997, **30**, 565.
- 30 (a) L. J. Barbour, X-SEED Version 2.0, Program for the Analysis of Single Crystal Structure Determinations, University of Stellenbosch, South Africa, 1999; (b) M. L. Connolly, Molecular Surface Package Version 3.9.3, Program for the Determination of Atom (Solvent) Accessible Areas and Volumes: see: M. L. Connolly, *J. Mol. Graphics*, 1993, **11**, 139.
- 31 J. L. Burmeister and F. Basolo, *Inorg. Chem.*, 1964, **3**, 1587.
- 32 (a) J. L. Burmeister, *Coord. Chem. Rev.*, 1966, **1**, 205; (b) J. L. Burmeister, *Coord. Chem. Rev.*, 1968, **3**, 225.
- 33 (a) M. J. Coyer, M. Croft, J. Chen and R. H. Herber, *Inorg. Chem.*, 1992, **31**, 1752; (b) M. J. Coyer, R. H. Herber, J. Chen, M. Croft and S. P. Szu, *Inorg. Chem.*, 1994, **33**, 716.
- 34 (a) C. Mantel, C. Baffert, I. Romero, A. Deronzier, J. Pecaut, M.-N. Collomb and C. Duboc, *Inorg. Chem.*, 2004, **43**, 6455; (b) S. A. Cotton, V. Franckevicius, R. E. How, B. Ahrens, L. L. Ooi, M. F. Mahon, P. R. Raithby and S. J. Teat, *Polyhedron*, 2003, **22**, 1489; (c) D. V. Naik and W. R. Scheidt, *Inorg. Chem.*, 1973, **12**, 272; (d) J. Rall, F. Weingart, D. M. Ho, M. J. Heeg, F. Tisato and E. Deutsch, *Inorg. Chem.*, 1994, **33**, 3442; (e) R. C. T. Rojo, L. Lezama, M. I. Arriortua, K. Urriaga and G. Villeneuve, *J. Chem. Soc., Dalton Trans.*, 1991, 1779.
- 35 F. A. Cotton, G. Wilkinson and P. L. Gaus, in *Basic Inorganic Chemistry*, Wiley Press, New York, 3rd edn, 1995, p. 98.
- 36 E. C. Constable, J. Lewis, M. C. Liptrot and P. R. Raithby, *Inorg. Chim. Acta*, 1990, **178**, 47.
- 37 J. S. Field, R. J. Haines, L. P. Ledwaba, R. McGuire, Jr., O. Q. Munro, M. R. Low and D. R. McMillin, *Dalton Trans.*, 2007, 192.
- 38 D. S. Martin, in *Extended Interactions between Metal Ions*, ed. L. V. Interante, ACS Symp. Ser. 5, American Chemical Society, Washington, DC, 1974, p. 254.
- 39 M. L. Connolly, *Science*, 1983, **221**, 709.
- 40 J. Hartung, I. Svoboda and M. T. Duarte, *Acta Crystallogr., Sect. C*, 1997, **53**, 1631.
- 41 D. R. McMillin and J. J. Moore, *Coord. Chem. Rev.*, 2002, **229**, 113.
- 42 J. F. Michael, S. A. Bejune, D. G. Cuttall, G. C. Summerton, J.-A. Gertenbach, J. S. Field, R. J. Haines and D. R. McMillin, *Inorg. Chem.*, 2001, **40**, 2193.
- 43 M. H. Wilson, L. P. Ledwaba, J. S. Field and D. R. McMillin, *Dalton Trans.*, 2005, 2754.
- 44 A. Islam, N. Ikeda, K. Nozaki, Y. Okamoto, B. Gholamkhash, A. Yoshimura and T. Ohno, *Coord. Chem. Rev.*, 1986, **171**, 355.
- 45 (a) K.-T. Yam, C.-M. Che and K.-C. Cho, *J. Chem. Soc., Dalton Trans.*, 1991, 1077; (b) H. Kunkely and A. Vogler, *J. Am. Chem. Soc.*, 1990, **112**, 5625; (c) V. M. Miskowski and V. H. Houlding, *Inorg. Chem.*, 1989, **28**, 1529.
- 46 S. C. F. Kui, S. S.-Y. Chui, C.-M. Che and N. Zhu, *J. Am. Chem. Soc.*, 2006, **128**, 8297.